Figure S1

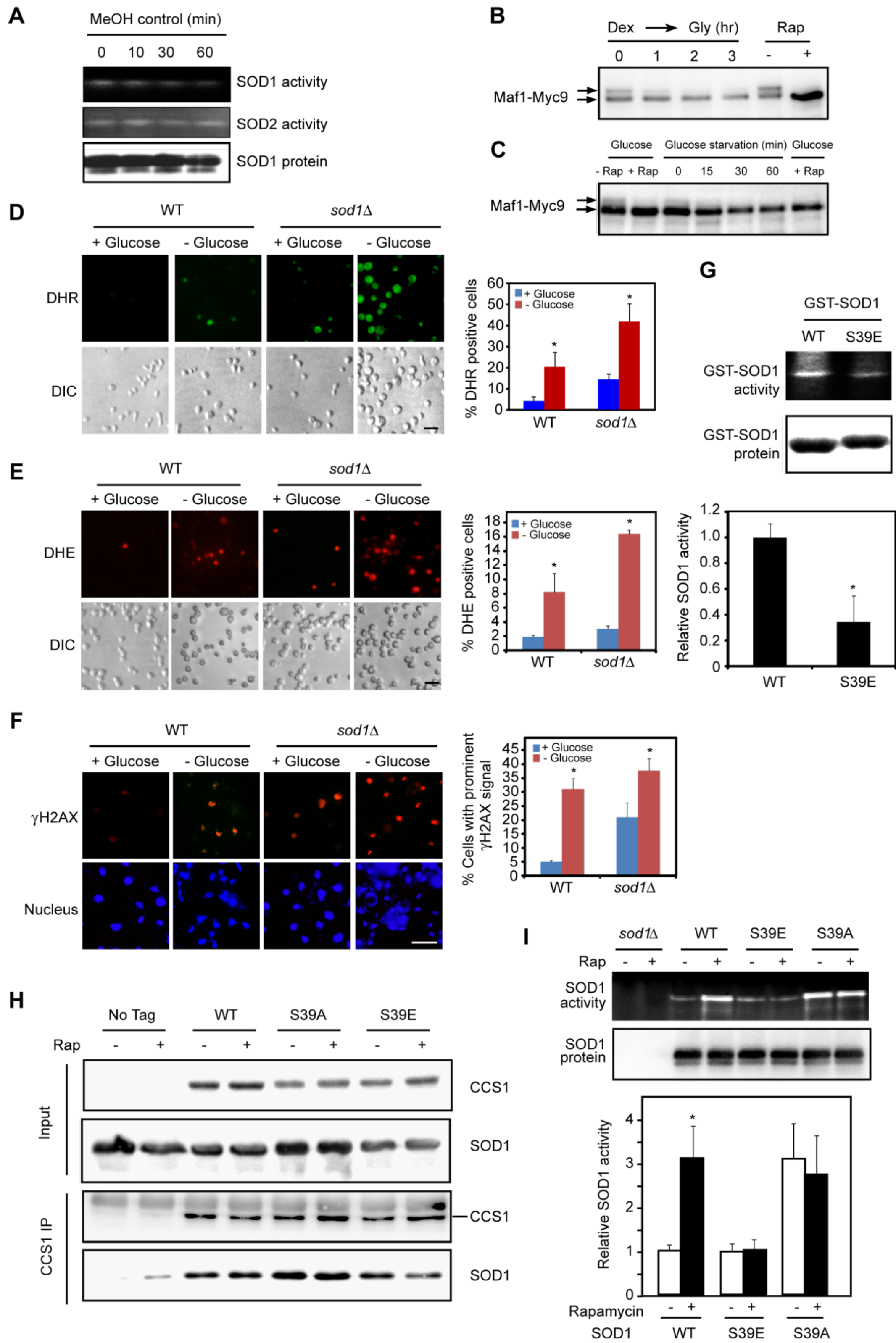

Figure S1. SOD1 is important for preventing excessive ROS accumulation and DNA damage under glucose starvation condition (related to Figure 1-3)

(A) MeOH solvent does not significantly affect SOD1 and SOD2 activity. Yeast cells were treated with solvent control (MeOH) for different times and the activity of SOD1 and SOD2 were examined by the in-gel SOD activity assay.

(B) Changing from glucose to non-fermentable carbon source inhibits TORC1 signaling. WT yeast cell culture was changed from glucose to glycerol medium for different times. TORC1 signaling was determined by MAF1-Myc9 phosphorylation as indicated by MAF1 electrophoretic mobility. Rapamycin (Rap, 100 nM, 30 min) was used as a control.

(C) Glucose starvation inhibits TORC1 signaling in a time-dependent manner. WT yeast cells were starved from glucose (SC without glucose) for different times. TORC1 signaling was determined by MAF1-Myc9 electrophoretic mobility shift.

(D) Glucose starvation causes elevated ROS in a SOD1-dependent manner. WT and *sod1*Δ cells cultured in glucose medium were changed to glucose-free medium for 1 hr. Cellular ROS were analyzed by staining with dihydrorhodamine (DHR). Images were captured by fluorescence microscopy. Scale bar, 10 μm. Right panel shows quantification of DHR-positive cells (mean ± S.D., n = 3, * $p < 0.05$, Student's *t*-test).

(E) Glucose starvation causes elevated superoxide in a SOD1-dependent manner. WT and *sod1*Δ cells were changed from glucose to glucose-free medium for 1 hr. Cellular superoxide was analyzed by staining with dihydroethidium (DHE). Images were captured by fluorescence microscopy. Right panel, quantification of DHE-positive cells (mean ± S.D., n = 3, * $p < 0.05$, Student's *t*-test). Scale bar, 10 μm.

(F) SOD1 is important for preventing DNA damage under glucose starvation conditions. DNA damage was analyzed by immunofluorescence (IF) with γ-H2AX antibody under the same conditions as in Figure S2C. Right panels show quantification of positively stained cells (mean ± S.D., n = 3, * $p < 0.05$, Student's *t*-test). Scale bar, 10 μm.

(G) S39E mutation suppresses the activity of bacterially expressed recombinant SOD1 protein. Bacterially expressed GST-SOD1^{WT} and GST-SOD1^{S39E} were subjected to in-gel SOD activity assay. Middle panel shows the protein loading by Coomassie blue staining. Lower panel, quantification of SOD1 activity. Data represent mean ± S.D. from three independent experiments (n = 3); * $p < 0.05$ compared with WT SOD1, Student's *t*-test.

(H) S39 phosphorylation does not affect the SOD1-CCS1 interaction. *sod1Δ CCS1-TAP* strains expressing SOD1^{WT}-Myc9, SOD1^{S39A}-Myc9 or SOD1^{S39E}-Myc9 were treated with 100 nM rapamycin for 1 hour. CCS1-TAP was affinity purified and the bound SOD1 was assayed by immunoblot with anti-TAP and anti-Myc antibodies. A strain with untagged CCS1 was used as a negative control.

(I) Activity of SOD1^{S39A} and SOD1^{S39E} mutants do not respond to rapamycin. *sod1Δ* strain expressing SOD1^{WT}-Myc9, SOD1^{S39A}-Myc9 or SOD1^{S39E}-Myc9 was treated with 100 nM rapamycin for 1 hour. SOD1 activity was assayed by the in-gel assay. Lower panel shows quantification of the results. Data represent mean ± S.D. from three independent experiments (n = 3); * $p < 0.05$, Student's *t*-test.

Figure S2

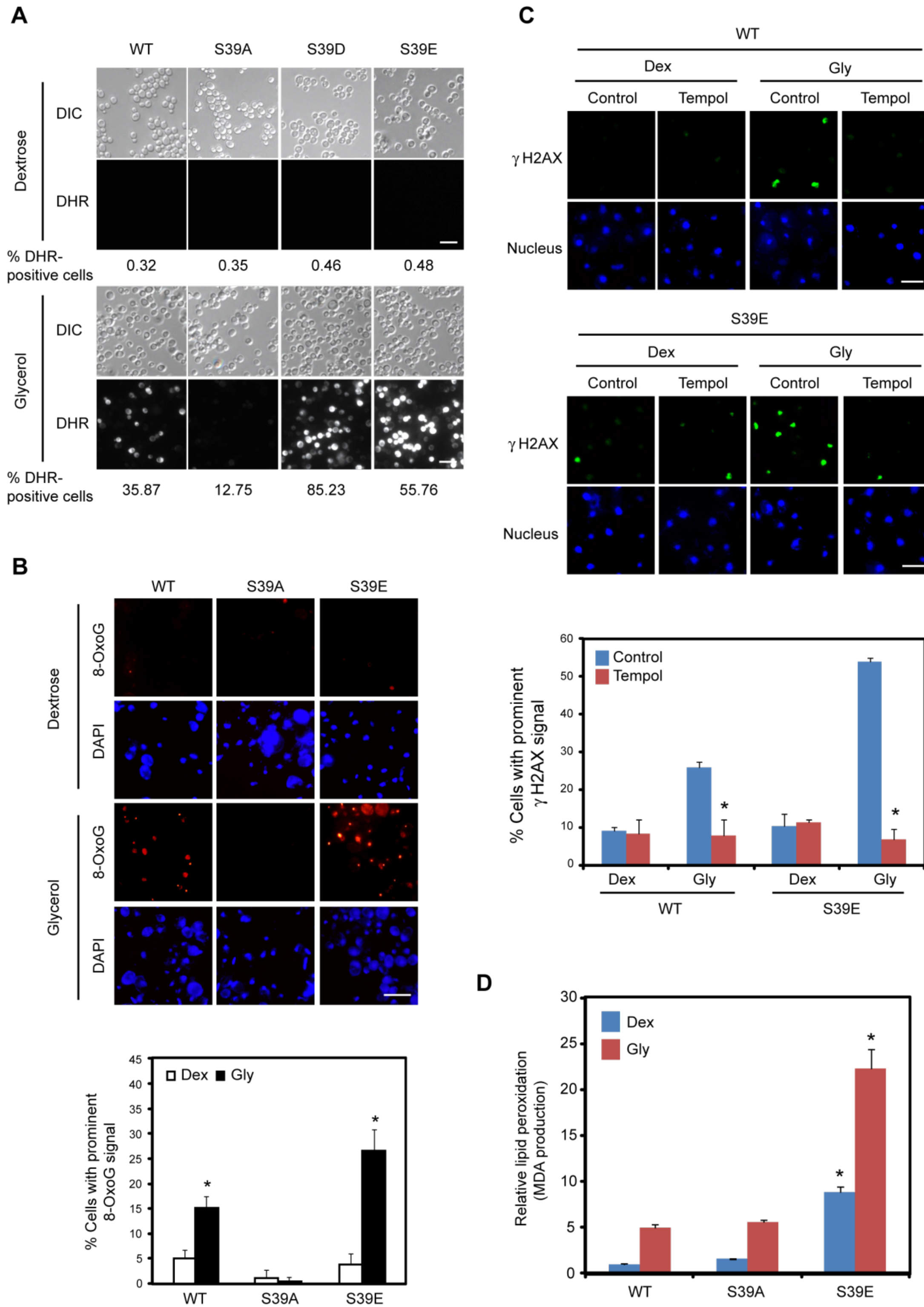

Figure S2. S39 phosphorylation is important for SOD1 to control cellular ROS and prevent oxidative DNA damage in response to changing nutrient conditions (related to Figure 4 &6)

(A) Yeast cells expressing WT and mutant SOD1 cultured in glucose were changed to glycerol medium for 3 hrs. Cellular ROS was analyzed by DHR staining. Quantification of results ($N > 100$) shows the % of DHR-positive cells. Scale bar, 10 μm.

(B) Yeast cells expressing WT and mutant SOD1 were changed from glucose to glycerol medium and incubated for 3 hr. DNA oxidative damage was analyzed by IF with 8-OxoG antibody (red). Nuclei were visualized by DAPI (blue). Dex, dextrose; Gly, glycerol. Scale bar, 10 μm. Right panel, data represent mean ± S.D. from three independent experiments ($N > 100$). * $p < 0.05$, Student's *t*-test.

(C) Tempol attenuates the effect of $SOD1^{S39E}$ mutation on DNA damage. Yeast cells expressing WT and S39E mutant SOD1 were changed from glucose to glycerol medium, and incubated for 3 hr in the absence (control) or presence of 50 μM Tempol. DNA damage was analyzed by IF with γ-H2AX antibody (green). Nuclei were visualized by DAPI (blue). Dex, dextrose; Gly, glycerol. Scale bar, 5 μm. Lower panel, quantification of γ-H2AX staining results. Data represent mean ± S.D of three independent experiments. * $p < 0.05$, Student's *t*-test ($N = 200$).

(D) SOD1 phosphorylation affects lipid peroxidation in yeast cells under different nutrient conditions. Yeast cells expressing WT and mutant SOD1 were changed from glucose to glycerol medium for 3 hrs. Cellular lipid peroxidation was analyzed by the Lipid Peroxidation (MDA) Assay. Results were quantified by the production of MDA relative to that of WT cultured in dextrose medium. Data represent mean ± S.D. from three independent experiments. * $p < 0.05$, Student's *t*-test.

Figure S3

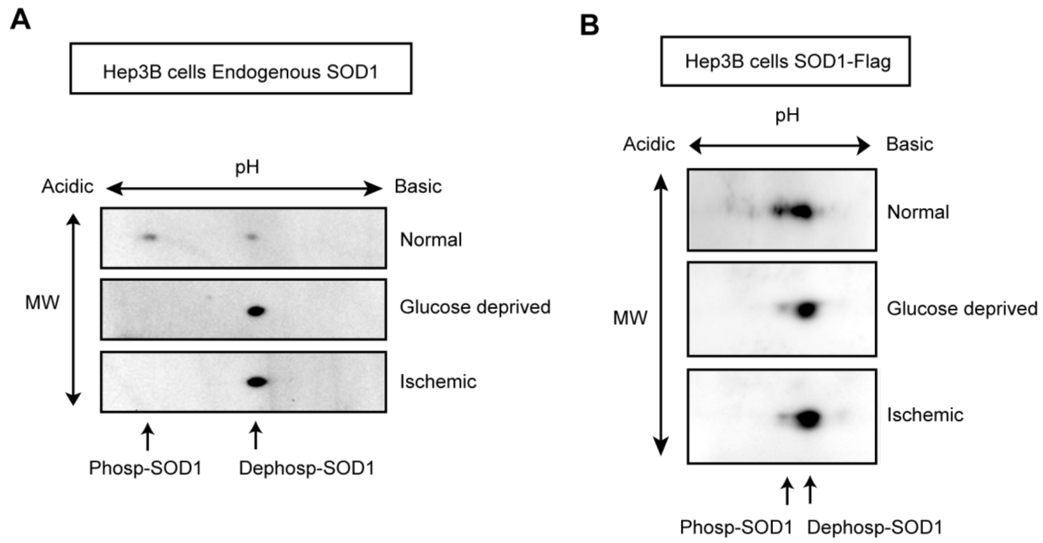

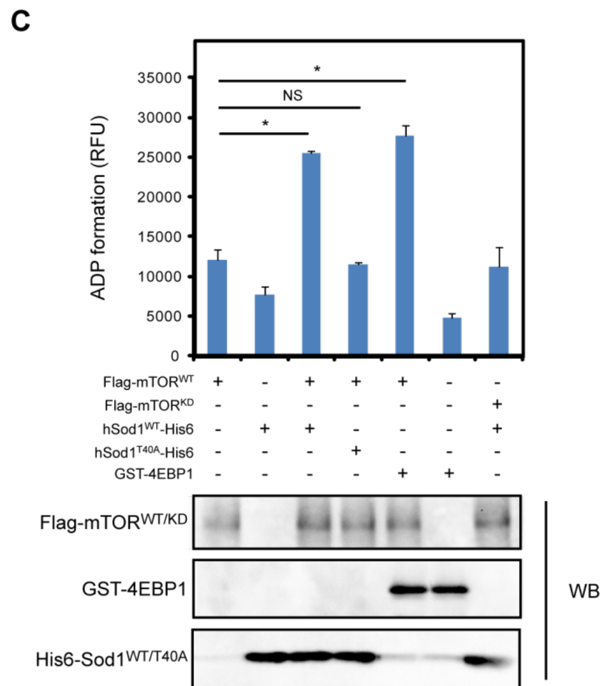

Figure S3. Glucose starvation leads to dephosphorylation of SOD1 (related to Figure 5)

(A) Hep3B cells were cultured under normal, glucose starvation or ischemic condition for 6 hours. Endogenous SOD1 protein was analyzed by 2D gel electrophoresis and immunoblot using anti-SOD1 antibody.

(B) Hep3B cells stably expressing $SOD1^{WT}$-Flag were cultured under normal, glucose starvation or ischemic condition for 6 hours. The SOD1-Flag proteins were analyzed by 2D gel electrophoresis and immunoblot using anti-Flag antibody.

(C) mTOR phosphorylates human SOD1 at T40 in vitro. Bacterially produced recombinant human His6-$SOD1^{WT}$, His-$SOD1^{T40A}$ or GST-4EBP1 was incubated for 30 min with Flag-$mTOR^{WT}$ or kinase dead Flag-$mTOR^{KD}$ expressed in HEK293FT cells and isolated by immunoprecipitation. SOD1 phosphorylation was determined by ADP production with the fluorometric kinase assay. Upper panel, quantification of ADP production by fluorometric measurement at Ex540 nm/Em590 nm. Data represent mean ± S.D. ($n=3$, * $p < 0.05$, Student's *t*-test). RFU, relative fluorescence unit. Lower panel, loading of mTOR and substrates determined by Western blot using anti-Flag, anti-4EBP1 or anti-His (Penta-His) antibodies.

Figure S4

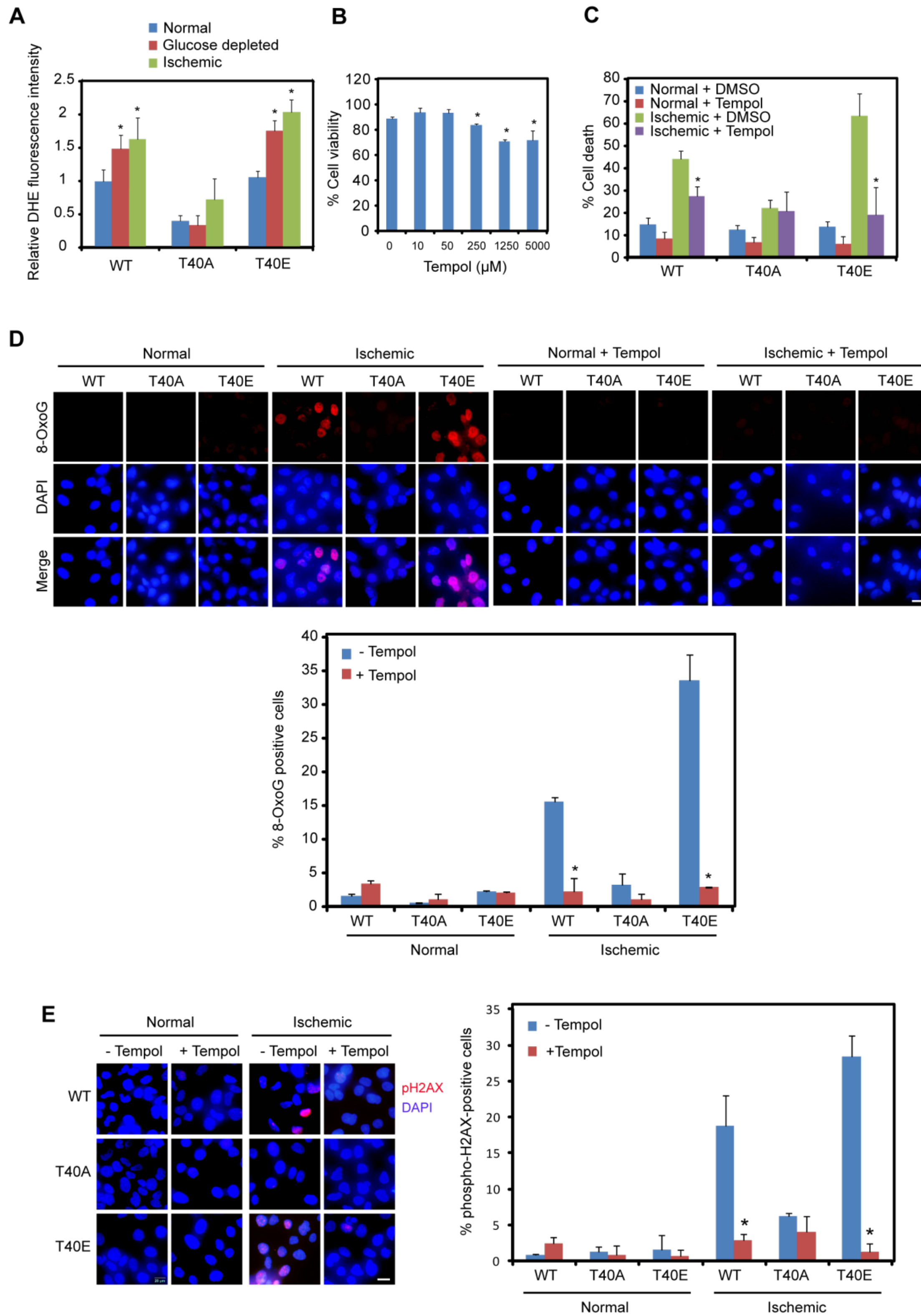

Figure S4. Glucose starvation causes elevated superoxide in Hep3B cells (related to Figure 6)

(A) Hep3B cells stably expressing $SOD1^{WT}$-GFP, $SOD1^{T40A}$-GFP and $SOD1^{T40E}$-GFP were incubated under normal, glucose starvation or ischemia for 6 hours. Superoxide was measured by DHE staining and flow cytometry. Data represent mean ± S.D. ($n = 3$, * $p < 0.05$, Student's *t*-test).

(B) Effect of different Tempol concentrations on Hep3B cells under normal culture condition. Hep3B cells stably expressing WT SOD1 were treated with different concentrations of Tempol for 24 hours. Cell death was assayed by Trypan blue staining. Data represent mean ± S.D. ($N = 3$, * $p < 0.05$, Student's t-test).

(C) Tempol attenuates Hep3B cell death during ischemia. Hep3B cells stably expressing $SOD1^{WT}$-GFP, $SOD1^{T40A}$-GFP and $SOD1^{T40E}$-GFP were pretreated with or without 50 μM Tempol for 1 hour and then subjected to ischemia for 24 hours in the absence or presence of 50 μM Tempol. Cell death was analyzed by Trypan blue staining. Data represent mean ± S.D. ($n = 3$, *$p < 0.05$, Student's *t*-test).

(D) Tempol attenuates DNA oxidation under ischemia. Hep3B cells stably expressing $SOD1^{WT}$-GFP, $SOD1^{T40A}$-GFP and $SOD1^{T40E}$-GFP proteins were pretreated with or without 50 μM Tempol for 1 hour, and then subjected to ischemia for 3 hours in the absence or presence of 50 μM Tempol. Oxidative DNA damage was analyzed by immunofluorescence staining with an 8-OxoG antibody. Scale bar, 20 μm. Lower panel, quantification of results. Data represent mean ± S.D. ($N = 3$, * $p < 0.05$, Student's *t*-test).

(E) Tempol attenuates DNA damage in an ischemic environment. Cells were treated as in (D) and analyzed for DNA damage by immunofluorescence staining with a p-H2A.X(S139)-specific antibody. Scale bar, 20 μm. Right panel, quantification of results. Data represent mean ± S.D. ($N = 3$, * $p < 0.05$, Student's *t*-test).

Figure S5

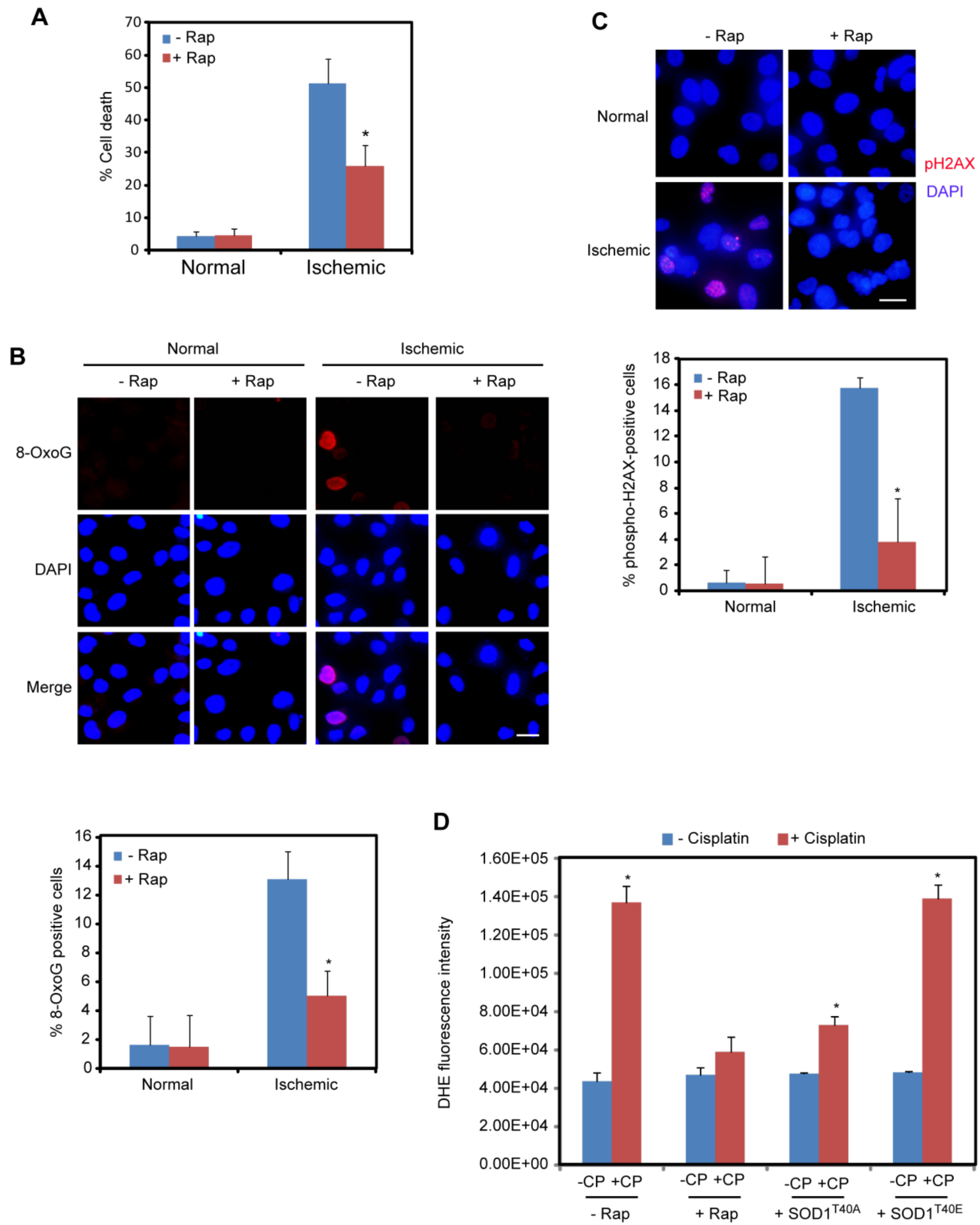

Figure S5. Rapamycin attenuates cancer cell death and oxidative DNA damage under ischemic environment (related to Figure 6)

(A) Hep3B cells expressing WT SOD1 under normal or ischemic condition in the absence or presence of 10 nM rapamycin (Rap) were assayed for cell death by Trypan blue staining. Data represent mean ± S.D. ($n = 3$, *$p < 0.05$, Student's *t*-test).

(B) Rapamycin attenuates DNA oxidation in an ischemic environment. Hep3B cells expressing WT SOD1 were pre-treated with or without 10nM rapamycin for 1 hour, then subjected to ischemia for 3 hours and analyzed for oxidative DNA damage by immunofluorescence staining with an 8-OxoG antibody. Scale bar, 20 µm. Right panel, quantification of 8-OxoG staining. Data represent mean ± S.D. ($n = 3$, * $p < 0.05$, Student's *t*-test).

(C) Cells in (B) were also analyzed for DNA damage by immunofluorescence staining with a p-H2A.X(S139)-specific antibody. Scale bar, 20 µm. Right panel, quantification of p-H2A.X(S139) staining. Data represent mean ± S.D. ($n = 3$, * $p < 0.05$, Student's *t*-test).

(D) Rapamycin attenuates cisplatin-induced superoxide production. Hep3B cells stably expressing $SOD1^{WT}$-GFP, $SOD1^{T40A}$-GFP and $SOD1^{T40E}$-GFP were treated with or without 10 µM cisplatin (CP) for 72 hours. Hep3B cells stably expressing $SOD1^{WT}$-GFP were also pre-incubated with 10 nM rapamycin for 30 min prior to treatment with or without 10 µM cisplatin (CP) for 72 hours. Superoxide was determined by DHE staining and flow cytometry. Data represent mean ± S.D. ($n = 3$, * $p < 0.05$, Student's *t*-test).

Figure S6

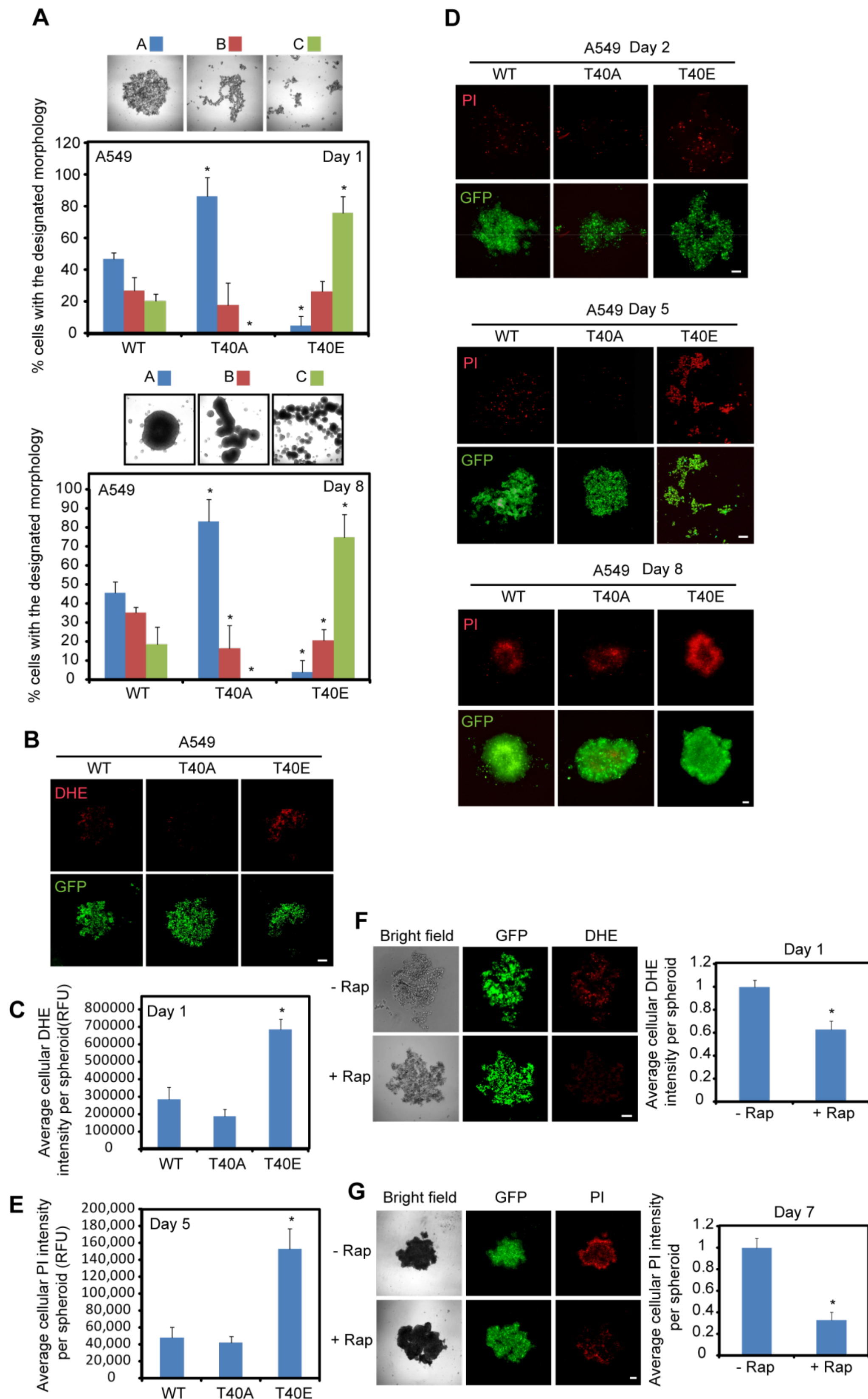

Figure S6. Activation of SOD1 enhances A549 tumor spheroid growth and survival (related to Figure 7)

(A) Activation of SOD1 enhances tumor spheroid formation. A549 cells stably expressing WT and mutant SOD1-GFP proteins were assayed for spheroid formation. Three typical tumor spheroid morphologies were quantified: A, complete tumor spheroid; B, incomplete tumor spheroid; C, dispersed tumor spheroid. Data represent mean ± S.D. of three independent experiments (N = 18 in each experiment, * $p < 0.05$, Student's *t*-test).

(B) Activation of SOD1 reduces superoxide level in tumor spheroids. Tumor spheroids derived from A549 cells stably expressing different SOD1-GFP proteins (green) were stained for DHE (red). Shown are representative microscopic images. Scale bar, 100 μm.

(C) Quantification of the DHE staining results in (B). Each spheroid was dissociated and the average cellular DHE intensity was measured by flow cytometer. Data represent mean ± S.D. (n=3, * $p < 0.05$, Student's *t*-test).

(D) Activation of SOD1 reduces cancer cell death in tumor spheroids. Tumor spheroids derived from A549 cells stably expressing different SOD1-GFP proteins (green) were analyzed for cell death by propidium iodine (PI) staining (red) at the indicated time points. Shown are representative microscopic images. Scale bar, 100 μm.

(E) Quantification of the PI staining results at day 5. Each spheroid was dissociated and the average cellular PI intensity was measured by flow cytometer. Data represent mean ± S.D. (n=3, * $p < 0.05$, Student's *t*-test).

(F) Rapamycin attenuates superoxide production and cell death in A549 tumor spheroids. Tumor spheroids derived from A549 cells stably expressing WT SOD1-GFP proteins (green) were treated with or without 10 nM rapamycin for 24 h prior to DHE staining. Shown are representative microscopic images at day 1 of spheroid culture. Scale bar, 100 μm. Right panel, quantification of the DHE staining relative to control. Each spheroid was dissociated and the average cellular DHE intensity was measured by flow cytometer. Data represent mean ± S.D. (n=3, * $p < 0.05$, Student's *t*-test).

(G) Tumor spheroids derived from A549 cells stably expressing WT SOD1-GFP proteins (green) were cultured in the absence or presence of 10 nM rapamycin. Shown are representative microscopic images. Cell death was analyzed by propidium iodine (PI) staining (red). Scale bar, 100 μm. Right panel, quantification of the PI staining relative to control. Each spheroid was dissociated and the average cellular PI intensity was measured by flow cytometer. Data represent mean ± S.D. (n=3, * $p < 0.05$, Student's *t*-test).

Table S1. Mass spectrometry analysis of SOD1 phosphorylation (related to Figure 3)

Sequence	Position of p-S/T	Rapamycin-sensitivity
VQAVAVLKGDAGVSGVVK	S15	0
GDAGVSGVVK	S15	0
FEQASESEPTTVSYEIAGNSPNAER	S24, S26, S39	1
GDAGVSGVVKFEQASESEPTTVSYEIAGNSPNAER	S15, S24, S39	1
GFHIHEFGDATNGcVSAGPHFNPFK	T55, S60	0
GFHIHEFGDATNGcVSAGPHFNPFKK	T55, S60	0
THGAPTDEVRHVGDmGNVK	T71, T76	0
HVGDMGNVKTDENGVAK	T90	0
TDENGVAKGSFK	T90	0
GSFKDSLIK	S99, S103	0
DSLIKLIGPTSVVGR	T111, S112	0
LIGPTSVVGR	T111, S112	0
LIGPTSVVGRSVVIHAGQDDLGK	T111, S112, S117	0
SVVIHAGQDDLGK	S117	0
SVVIHAGQDDLGKGDTEESLK	S117, T132, S135	0
TGNAGPRPAcGVIGLTN	T138	0

0, Not affected by rapamycin
1, Inhibited by rapamycin